*Proceedings of the 2024 Winter Simulation Conference*
*H. Lam, E. Azar, D. Batur, S. Gao, W. Xie, S. R. Hunter, and M. D. Rossetti, eds.*

# FLOOD SCENARIO GENERATION USING THE NORTA MODEL

Ashutosh Shukla[1], John Hasenbein[1], and Erhan Kutanoglu[1]

[1]Graduate Program in ORIE, The University of Texas at Austin, Austin, TX, USA

## ABSTRACT

Several stochastic programming models have been developed for critical infrastructure's resilience decision-making to extreme flood events. Generating flood scenarios for such models requires running advanced flood models on a sophisticated computing infrastructure for different parameterizations (for example, different hurricane intensity levels, tracks, etc.), which may not always be practical. To address this issue, in this study, we propose a Normal-to-Anything (NORTA) model-based flood scenario generation scheme, which requires significantly fewer computing resources. The scenarios we generate using the proposed approach preserve correlation in flood height at locations of interest, in our case, the power transmission grid's substation locations. We demonstrate our approach's efficacy with a case study using a synthetic power grid with statistical similarities with the actual Texas grid and the flood maps developed by the National Atmospheric and Oceanic Administration that represent the storm-surge risk in Texas.

## 1 INTRODUCTION

In the past four decades, the U.S. has experienced 377 weather and climate disasters where the cost for each event exceeded \$1B, and these events have collectively inflicted losses of over \$2.67T (Smith 2024). To minimize this loss in the future, enhancing the resilience of critical infrastructure to such extreme events has become the government's priority.

Simultaneously, several studies such as (Logan et al. 2022) and (Watson et al. 2014) have introduced conceptual frameworks to assess and enhance the resilience of a system. Both studies acknowledge that the notion of resilience should be system and threat-specific. Watson et al. propose that a system's resilience decision-making should consider the nature of the threat, its impact on the system, and the likelihood of it occurring. One popular way of doing this is by representing the threat using a set of scenarios. For example, in the case of Hurricane Harvey, flooding scenarios associated with hypothetical but plausible hurricane tracks, each having a different landfall location (to represent the track uncertainty), are generated using an in-land flooding model in (Kim et al. 2021). The use of scenarios representing an extreme weather event to assess the damage that the event can potentially cause to public life and property is shown in (Souto et al. 2022) and (Miura et al. 2021). Both studies focus on risk assessment and resilience planning of a critical infrastructure against extreme flooding. Moreover, they both rely on physics-based flood prediction models. These models have an advantage over other commonly used statistical models (which we review in Section 2) because they can preserve pair-wise correlation in flood height across different locations. While physics-based flood models are precise and accurate, they require sophisticated computing infrastructure and may take several hours to produce the desired output.

This study demonstrates how a statistical model referred to as the Normal-to-Anything (NORTA) model (see (Cario and Nelson 1997)) can generate flood scenarios in a much more computationally tractable way that can preserve pair-wise correlations in flood height. Specifically, we make the following contributions:

1. We review the NORTA model introduced in (Cario and Nelson 1997) and implement it in Python for flood scenario generation. While doing so, we address a shortcoming of the model that is highlighted

in (Ghosh and Henderson 2003), using a semi-definite programming-based augmentation technique proposed in the same article.

2. We use our implementation to generate flood scenarios for storm-surge flooding. Towards this goal, we leverage the output of the completed runs of a sophisticated physics-based flood prediction model to generate input for the NORTA model. The specific output of the physics-based model used for the NORTA implementation represents the storm-surge flood risk in Texas.

The rest of the paper is organized as follows. We dedicate Section 2 to reviewing various scenario generation methods and Section 3 to discussing the NORTA method and its implementation. Section 4 describes how we use NORTA to generate flood scenarios. Finally, in Section 5, we summarize our findings and suggest a direction for future research.

## 2 LITERATURE REVIEW

We broadly classify scenario-generation techniques into four categories. The first set of methods is based on fragility curves. These curves are cumulative distribution functions representing the failure probability of a component as a function of a load parameter. Such curves are used in civil engineering applications and have been developed for buildings (Rota et al. 2010), bridges (Kim and Shinozuka 2004), and tunnels (Andreotti and Lai 2019). They also have been developed for several power system components like transmission towers (Panteli et al. 2017). It is important to note that these curves represent risk for a single component and do not capture the system-wide impact of simultaneous failure of different components within the same system. This is usually not an issue in civil engineering applications where the collapse of one building cannot cause disruptions in the functioning of another building. In power systems, however, failure of a component has network effects and disrupts the functioning of other parts of the network due to the complex power flow physics. Therefore, for such applications, we need methods to augment fragility curves by accounting for correlated failure effects.

The second set of methods is physics-based, such as hydrology-driven flood estimation models. These models take various meteorological inputs, such as precipitation intensity and the region's digital elevation data, to generate a correlated flood map associated with the inputs. Two popular models that fit this framework and that are extensively used for flood forecasting are WRF-Hydro (Gochis et al. 2020) (for precipitation-induced inland flooding) and SLOSH (Glahn et al. 2009) (for storm-surge forecasting). Such models capture correlations in flood height, which is crucial for resilience assessment and planning for critical infrastructures like the power grid where network effects exist. However, these models require sophisticated computing infrastructure and expertise in running them, which are both hard to access.

The third set of methods uses statistical and data-driven models. These models rely on past observation data to estimate a statistical model further used for scenario generation. Such models have been used for transmission expansion planning with high renewable energy penetration (Sun et al. 2018), to generate scenarios for wind power forecasting (Ma et al. 2013), and predicting track and intensity of typhoons (Rüttgers et al. 2022). Statistical models offer an advantage over physics-based models because they may not require significant computational resources. However, this advantage comes at the cost of being a low-fidelity model that may not capture higher-order correlations.

The fourth set of methods explores the combinatorial space of possible failures to generate scenarios. The $N-k$ criterion commonly used in the power system reliability literature is based on this approach. The criteria assess the system's reliability when $k$ out of $N$ components fail simultaneously. The decision-making models that use such criteria typically aim to ensure robustness under worst-case scenarios (when the $k$ most critical components go out of order). The decision-making models based on $N-k$ criteria have been developed for unit commitment decision-making in (Wang et al. 2013) and (Street et al. 2011) and for power system's resilience planning (Bagheri and Zhao 2019) and (Che et al. 2018). Using such scenarios is popular in reliability studies as failures can reasonably be assumed to be independent. Furthermore, such models recommend conservative decisions for large values of $k$.

The proposed NORTA model-based approach in this study can be classified in the third category (statistics-based and data-driven). The NORTA model was first proposed in (Cario and Nelson 1997) and several methodological developments related to the model have been made since (Chen 2001), (Ghosh and Henderson 2003), and (Ghosh and Pasupathy 2011). The literature on the application of the NORTA model, however, is scant. In finance, the model has been used to model portfolio credit risk in (Ayadi et al. 2019) and to simulate investment returns in (Morton et al. 2006). The model has also been used in computational biology for generating synthetic datasets in (Kurtz et al. 2015) and to assess the performance of metrics that infer global properties of biological networks in (Villani et al. 2018). For energy systems, a framework similar to ours, an analysis based on the NORTA model has been developed in (Wadman et al. 2017). The model, however, is developed to forecast the energy generated from intermittent sources like wind and solar, which is not the focus of our study.

## 3 MODELING

NORTA is a model to represent an $n$-dimensional multivariate random vector $\mathbf{X} = (X_1, X_2, \ldots, X_n)$ with arbitrary marginal distributions and a feasible correlation matrix. The input to the model consists of two components: (a) the marginal distribution $F_{X_i}$ of the random variable $X_i$ for $i = 1, 2, \ldots, n$, and (b) the $n \times n$ correlation matrix $\sum_\mathrm{X}$ of the random vector $\mathbf{X}$. The model outputs $n$-dimensional random samples that adhere to the specified marginal distributions of the elements of $\mathbf{X}$ and the correlation matrix of $\mathbf{X}$. We split further discussion on NORTA modeling into two parts. The first part focuses on the key properties of the transformation function used in NORTA and how we estimate the parameters of the NORTA model. The subsequent part describes generating random samples of $\mathbf{X}$.

### 3.1 Parameter estimation

In the NORTA model, we transform a base random vector $\mathbf{Z}$, which follows a multivariate normal distribution with a known correlation matrix to obtain the marginal distributions of the input vector $\mathbf{X}$. Specifically, $\mathbf{X}$ is represented as:

$$\mathbf{X} = \begin{bmatrix} F_{X_1}^{-1}[\Phi(Z_1)] \\ F_{X_2}^{-1}[\Phi(Z_2)] \\ \cdot \\ \cdot \\ \cdot \\ F_{X_n}^{-1}[\Phi(Z_n)] \end{bmatrix}. \tag{1}$$

In equation (1), $\Phi$ represents the univariate standard normal cumulative distribution function, and $F_X^{-1}(u) \equiv \inf\{x : F_X(x) \geq u\}$ represents the inverse of the cumulative distribution function for a random variable $X$. Such a transformation ensures that the marginal distribution of the elements of $\mathbf{X}$ when estimated from the generated samples remain consistent with the input data. The correlation between the pairs of elements of $\mathbf{X}$ is preserved in the generated samples by appropriately adjusting the correlation values between pairs of elements of $\mathbf{Z}$. To understand how to adjust these values, recall that the correlation between two variables, $X_i$ and $X_j$, is given by:

$$\mathrm{Corr}(X_i, X_j) = \frac{\mathrm{E}(X_i X_j) - \mathrm{E}(X_i)\mathrm{E}(X_j)}{\sqrt{\mathrm{Var}(X_i)\mathrm{Var}(X_j)}}. \tag{2}$$

In equation (2), all the terms on the right-hand-side except $\mathrm{E}[X_i X_j]$ can be inferred from the marginal distributions of $X_i$ and $X_j$, which in the case of NORTA modeling are provided as input. Using equation

(1), the term $\mathrm{E}[X_i X_j]$ can be expressed as:

$$\begin{aligned}\mathrm{E}[X_i X_j] &= \mathrm{E}[F_{X_i}^{-1}[\Phi(Z_i)]F_{X_j}^{-1}[\Phi(Z_j)]] \\ &= \int_{-\infty}^{\infty}\int_{-\infty}^{\infty} F_{X_i}^{-1}[\Phi(Z_i)]F_{X_j}^{-1}[\Phi(Z_j)]\phi(Z_i,Z_j)dZ_i dZ_j.\end{aligned} \tag{3}$$

The term $\phi(Z_i,Z_j)$ in the right-hand-side of equation (3) represents the probability density function of the standard bivariate normal distribution, which is completely specified by the correlation between $Z_i$ and $Z_j$. We represent this correlation value by $\rho_Z(i,j)$. From equations (2) and (3), we infer that the correlation between variables $X_i$ and $X_j$ (represented by $\rho_X(i,j)$) can be characterized by $\rho_Z(i,j)$. Let $c_{ij} : \mathbb{R} \mapsto \mathbb{R}$ be a transformation such that

$$c_{ij}[\rho_Z(i,j)] = \rho_X(i,j).$$

In (Cario and Nelson 1997), the authors highlight four important characteristics of the function $c_{ij}$:

1. $c_{ij}[0] = 0$ and $\rho_Z(i,j) \geq 0$ implies that $c_{ij}[\rho_Z(i,j)] \geq 0$. Similarly, $\rho_Z(i,j) \leq 0$ implies that $c_{ij}[\rho_Z(i,j)] \leq 0$.
2. If $\bar{\rho}_{ij}$ and $\underline{\rho}_{ij}$ are maximum and minimum feasible correlation values for random variables $X_i$ and $X_j$, then $c_{ij}[1] = \bar{\rho}_{ij}$ and $c_{ij}[-1] = \underline{\rho}_{ij}$.
3. The function $c_{ij}[\rho_Z(i,j)]$ is non-decreasing for $-1 \leq \rho_Z(i,j) \leq 1$.
4. Under mild conditions, the function $c_{ij}[\rho_Z(i,j)]$ is continuous in [-1,1].

These properties enable us to estimate the value of $\rho_Z(i,j)$ from $\rho_X(i,j)$ (which is an input) using a numerical line search procedure that can be run in parallel for different combinations of random variables to populate the correlation matrix for the base vector **Z**, which we refer to as $\Lambda_Z$. This matrix, however, can have an issue: it may not be positive semi-definite and, therefore, not a valid correlation matrix. This is an issue with the NORTA model; such matrices are referred to as NORTA-defective.

Through an empirical study, it is shown in (Ghosh and Henderson 2003) that the probability that a correlation matrix generated via the NORTA model is infeasible grows acutely with the dimension and is almost 1 when the dimension of the input vector is more than 15. In our application of the NORTA model for flood scenario generation, the size of the input vector is determined by the number of flooded substations which, in our case, is 72. Consequently, we end up with a NORTA-defective matrix after running the line search procedure. To address this issue, an approach to post-process $\Lambda_Z$ to make it feasible is proposed in (Ghosh and Henderson 2003). Specifically, the authors propose solving a semi-definite program that minimizes a norm ($L_2$, $L_1$, or $L_\infty$) between $\Lambda_Z$ and a target matrix Y such that the resulting matrix (Y) becomes positive semi-definite and, therefore, feasible. This version of the NORTA model is referred to as augmented-NORTA with the semi-definite program as follows:

$$\begin{aligned}\underset{Y\in\mathbb{R}^{n\times n}}{\text{minimize}} \quad & r(Y,\Lambda_Z), \\ \text{subject to} \quad & Y \succeq 0, \\ & Y[i,i] = 1, \ \forall \quad i = 1,\ldots,n.\end{aligned}$$

Here, $r(Y,\Lambda_Z)$ represents a distance measure between $Y$ and $\Lambda_Z$. In our implementation, we minimize the sum of $L_2$ distances between elements of the matrices. Specifically,

$$r(Y,\Lambda_Z) = \sum_{i=1}^{n}\sum_{j=1}^{n}(Y[i,j] - \Lambda_Z[i,j])^2,$$

where $n$ is the dimension of the input random vector **X**.

We highlight that the approach proposed above addresses the issue of NORTA-defectiveness. The input matrix $\sum_{\mathrm{X}}$ is assumed to be a feasible matrix, i.e., it is positive semi-definite and exists for the set of input marginal distributions. Whether a given correlation matrix is feasible for the given set of marginal distributions can be checked using the computational procedure described in (Ghosh and Henderson 2002).

### 3.2 Scenario generation

After we obtain the correlation matrix $Y$, we perform its Cholesky decomposition, which we represent as $Y = MM^T$. The generation of samples using $M$ is straightforward, with steps outlined in algorithm 1.

**Algorithm 1** Sampling using NORTA

1. **Input:** $M$, $m$
2. **Output:** A vector of size $m$
3. Initialize a vector $S$
4. $i \leftarrow 0$
5. **while** $i < m$ **do**
6. Generate $\hat{Z} = (Z_1, Z_2, \ldots, Z_n)$, where each element is i.i.d standard normal
7. Compute $Z = M\hat{Z}$
8. Compute $X = (X_1, X_2, \ldots, X_n)$ where $X_j = F_{X_j}^{-1}[\Phi(Z_j)]$ for all $j \in \{1, 2, \ldots, n\}$
9. $S \leftarrow S \cup \{X\}$ {Append $X$ to vector $S$}
10. $i \leftarrow i+1$
11. **end while**
12. **return** $S$

## 4 STORM SURGE FLOOD SCENARIO GENERATION

Flood scenario generation methods that can preserve the correlation between flooding at different locations have several applications in the resilience planning of critical infrastructures. We now discuss how the NORTA model can generate such correlated flood scenarios. To demonstrate this, we use flood maps generated by NOAA. These maps represent storm-surge risk in the Texas Gulf Coast region and are constructed by post-processing the output of the Sea, Lake, and Overland Surges from Hurricanes (SLOSH) model (Glahn et al. 2009). SLOSH is a physics-based storm-surge prediction method based on a parametric wind model. The wind model takes the storm's track, the radius of the maximum wind, and the pressure difference between the storm's central pressure and the ambient pressure as input. Then, the wind field is generated using these inputs, which induce surface stresses on the ocean surface beneath the hurricane, leading to a surge of water.

We use a composite product called the Maximum Envelope of Water (MEOW) (Zachry et al. 2015), developed by post-processing output of thousands of SLOSH runs based on hypothetical hurricanes with various combinations of intensity categories, forward speeds, track directions, and landfall locations that are representative of future storms that may hit the Texas coast. The map represented by the maximum flood values for each grid cell is referred to as a MEOW. An example MEOW map is shown in Figure 1.

In the original MEOW dataset for the Texas Gulf Coast region, there exist 192 different MEOW maps corresponding to different combinations of eight storm directions (west-south-west, west, west-north-west, north-west, north-north-west, north, north-north-east, and north-east), six intensity categories (0-5), and four forward speeds (5, 10, 15, and 25 mph). To demonstrate the usefulness of the proposed approach with a computationally tractable use case, we reduce the size of the problem by eliminating a subset of less severe scenarios. We first drop the MEOW maps corresponding to four directions (west-south-west, north, north-north-east, and northeast) as hurricanes belonging to these categories do not cause significant flooding

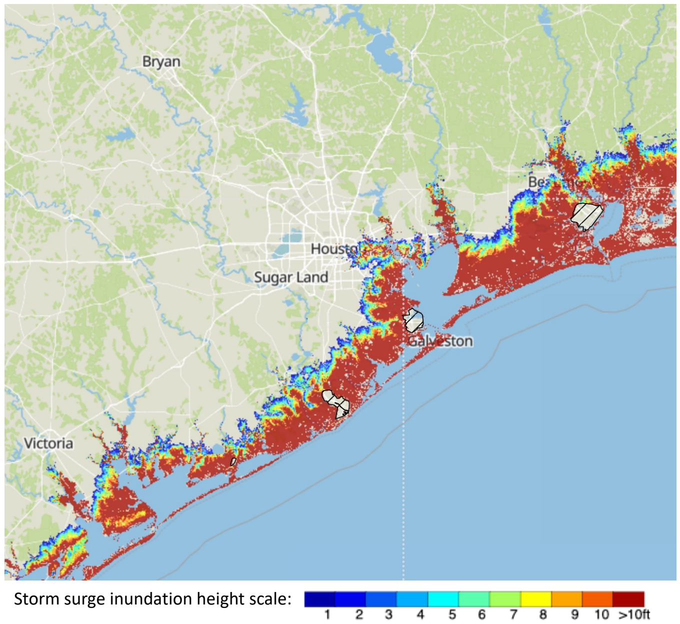


Figure 1: A sample MEOW generated using category 5 storms approaching the Texas Gulf Coast in the north-west direction with a forward speed of 5 mph.

in the Texas Gulf Coast. We also drop the MEOW maps corresponding to category 0-4 hurricanes. The storms belonging to category 5 are more intense versions of these storms. We overlay the maps we are left with on a reduced version of the synthetic power transmission grid (ACTIVSg2000) that shares statistical similarities with the actual Texas transmission grid (Birchfield et al. 2017). The network reduction on the original dataset is performed such that the nodes in the inland region, unaffected by the storm surge, are consolidated into a smaller set of nodes while the coastal part of the grid exposed to the Gulf of Mexico remains intact as in the original grid so that the coastal flood risk is fully taken into account. The reduced grid consists of 362 substations, of which 72 are flooded in at least one MEOW map. Figure 2 displays the impact of network reduction.

To generate input for the NORTA model, consider that flood height at substation $i$ in MEOW map $j$ represents a realization $j$ of element $i$ ($X_i$) of random vector $\mathbf{X}$ introduced in Section 3. Therefore, $\mathbf{X}^{(j)}$ in

$$\mathbf{X}^{(j)} = \begin{bmatrix} X_1^j \\ X_2^j \\ \cdot \\ \cdot \\ \cdot \\ X_n^j \end{bmatrix}$$

is a random sample which constitutes the flood height at substations in a power grid network for MEOW map $j$. We use 16 such samples, one for each MEOW map, to construct empirical cumulative distribution function for the marginal distribution of flooding at each flooded substation. Accordingly, $F_{Xi}$ represents a distribution over flood heights at substation $i$ across different MEOW maps. We note that random variables are defined only for those substations that are flooded in at least one MEOW. The correlation matrix, another input to the NORTA model, is developed using the same MEOWs. Since we consider these flood maps to represent the samples generated from the joint distribution of flooding, we estimate pairwise correlations

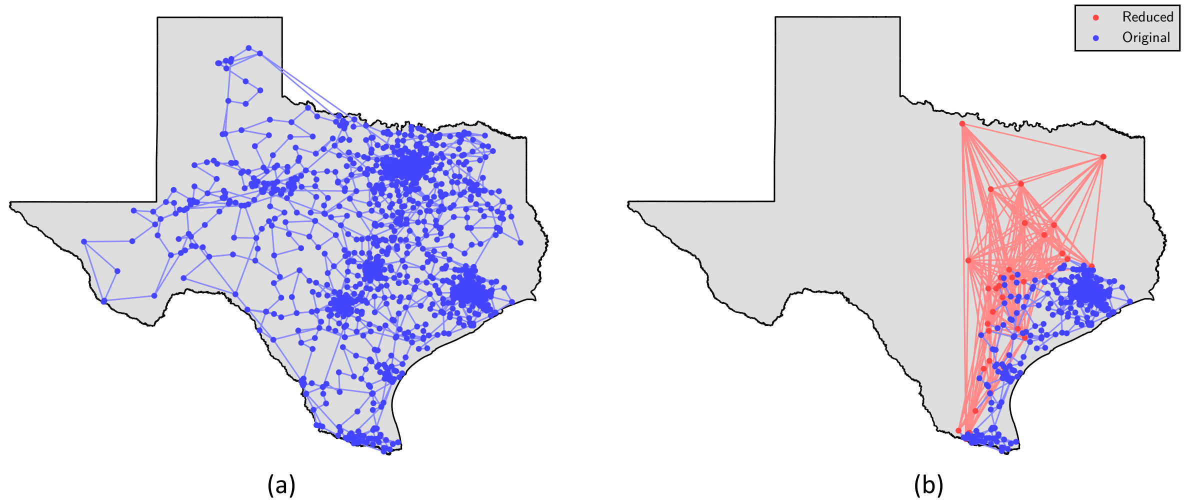


Figure 2: (a) The ACTIVSg2000 synthetic grid for Texas. (b) The reduced grid obtained after performing the network reduction. The red elements represent the new nodes and branches that were introduced as the artifacts of the reduction procedure to maintain equivalence in the grid characteristics.

for each pair of flooded substations, say substations $p$ and $q$ by estimating correlation between $X_p$ and $X_q$ using the 16 MEOW maps data. Figure 3 shows a schematic overview of our approach.

Given how the MEOW maps are generated, they have an inherent limitation; they represent an extreme case flood profile that any single hurricane may not realize. Nonetheless, this does not inhibit us from demonstrating the use of NORTA for correlated flooding scenarios as we focus on showing that input marginal distributions and correlation are preserved in the samples. The inputs can be replaced with marginals and correlation matrices generated from alternative flood models. In this sense, the NORTA model is agnostic to the flood model for constructing marginal distribution and the correlation matrix.

We now assess the performance of the NORTA model in terms of how well the samples generated from it adhere to the marginal distributions and the correlation matrix that we give as input to the model. To do so, for each marginal distribution, we compute the Earth mover's distance (EMD) for the univariate random variable $X_i$ as given by

$$EMD_i = \int_{-\infty}^{\infty} |F_{X_i} - \hat{F}_{X_i}|,$$

where $F_{X_i}$ represents the input marginal distribution, and $\hat{F}_{X_i}$ represents the marginal distribution of $X_i$ that we estimate from the NORTA samples. The EMD is a measure of the dissimilarity between the two probability distributions. We compute EMD for each input marginal distribution and present its average value, standard deviation, and specific quantiles in the Earth mover's distance column in Table 1. We highlight that for $n$ input samples, we can upper bound the EMD as:

$$\max(EMD_i) = \max(X_i^1, X_i^2, \cdots, X_i^n).$$

In our case study, $\max(EMD_i)$ lies between 1 and 21 for different $i$'s. With respect to these values, the mean and maximum EMD values that we calculate from our NORTA model in Table 1 are small.

Similarly, we present the value of the same statistics of error between the input pair-wise correlation and the pair-wise correlation value that we estimate from the NORTA samples in the Correlation error column of the same table. For error calculations in both cases, we generate 800 samples. The values in both columns suggest that the NORTA model generated correlated flood scenarios with high accuracy even in 72 dimensions.

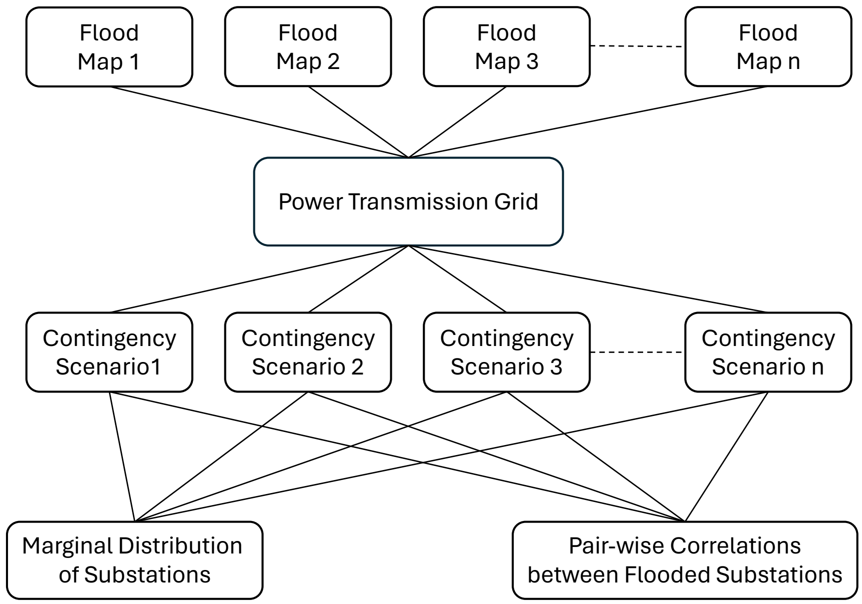


Figure 3: Schematic figure representing the steps to generate the input for the NORTA model. In the first step, we overlay the flood maps on the transmission grid to identify flooded substations in each contingency scenario. Next, we use these contingency scenarios to develop an empirical cumulative distribution function for the marginal distribution of substation flooding and to estimate pair-wise flooding correlation between substations.

Table 1: The Earth mover's distance column shows the value of the mean, standard deviation, and distribution across various percentiles for the Earth mover's distance between the input marginal distribution and the distribution estimated from the NORTA samples across 72 flooded substations. The correlation error column shows the same metrics for the difference between pair-wise correlations of the input correlation matrix and the correlation matrix estimated from the NORTA samples.

| | Earth mover's distance | Correlation error |
|---|---|---|
| mean | 0.073 | 0.041 |
| std | 0.038 | 0.038 |
| min | 0.001 | 0.000 |
| 25% | 0.052 | 0.013 |
| 50% | 0.071 | 0.030 |
| 75% | 0.103 | 0.058 |
| max | 0.146 | 0.329 |

## 5 CONCLUSIONS

This study aims to develop an efficient computational method for creating correlated flood scenarios. To achieve this goal, we assess the effectiveness of the NORTA model in generating such scenarios. Specifically, we create a Python-based implementation of the NORTA method outlined in (Cario and Nelson 1997) and (Ghosh and Henderson 2003). Using this implementation, we generate scenarios representing flood heights at 72 transmission grid substations in the Texas Gulf Coast region. We evaluate the NORTA method's performance by assessing its ability to produce samples that match the expected marginal distributions of flooding at individual substations, using the Earth mover's distance metric. Additionally, we measure the error between the empirical correlation values derived from the samples and the intended correlation values. As a future direction, we propose conducting case studies to compare the effectiveness of resilience planning decisions based on scenarios generated from the NORTA model against those derived from other commonly used methods, such as those relying on fragility curves.

## 6 ACKNOWLEDGEMENTS

We gratefully acknowledge the contribution of the NORTA implementation available as an open-source repository at https://github.com/dukduque/NortaPy, upon which our code base was developed.

## REFERENCES

Andreotti, G., and C. Lai. 2019. "Use of fragility curves to assess the seismic vulnerability in the risk analysis of mountain tunnels". *Tunnelling and Underground Space Technology* 91:103008.

Ayadi, M., H. Ben-Ameur, N. Channouf, and M. Gaha. 2019. "NORTA for portfolio credit risk". *Annals of Operations Research* 281:99–119.

Bagheri, A., and C. Zhao. 2019. "Distributionally robust reliability assessment for transmission system hardening plan under $N-k$ security criterion". *IEEE Transactions on Reliability* 68(2):653–662.

Birchfield, A. B., T. Xu, K. M. Gegner, K. S. Shetye, and T. J. Overbye. 2017. "Grid structural characteristics as validation criteria for synthetic networks". *IEEE Transactions on Power Systems* 32(4):3258–3265.

Cario, M., and B. L. Nelson. 1997. "Modeling and generating random vectors with arbitrary marginal distributions and correlation matrix". Technical report, Northwestern University. Online link: https://www.ressources-actuarielles.net/EXT/ISFA/1226.nsf/769998e0a65ea348c1257052003eb94f/5d499a3efc8ae4dfc125756c00391ca6/$FILE/NORTA.pdf (Accessed: 2024-08-21).

Che, L., X. Liu, and Z. Li. 2018. "Preventive mitigation strategy for the hidden $N-k$ line contingencies in power systems". *IEEE Transactions on Reliability* 67(3):1060–1070.

Chen, H. 2001. "Initialization for NORTA: generation of random vectors with specified marginals and correlations". *INFORMS Journal on Computing* 13(4):312–331.

Ghosh, S., and S. G. Henderson. 2002. "Chessboard distributions and random vectors with specified marginals and covariance matrix". *Operations Research* 50(5):820–834.

Ghosh, S., and S. G. Henderson. 2003. "Behavior of the NORTA method for correlated random vector generation as the dimension increases". *ACM Trans. Model. Comput. Simul.* 13(3):276–294.

Ghosh, S., and R. Pasupathy. 2011. "C-NORTA: a rejection procedure for sampling from the tail of bivariate NORTA distributions". *INFORMS Journal on Computing* 24(2):295–310.

Glahn, B., A. Taylor, N. Kurkowski, and W. Shaffer. 2009. "The role of the SLOSH model in National Weather Service storm surge forecasting". *National Weather Digest*:1–12.

Gochis, D. J., M. Barlage, R. Cabell, M. Casali, A. Dugger, K. FitzGerald, M. McAllister, J. McCreight, A. RafieeiNasab, L. Read, K. Sampson, D. Yates, and Y. Zhang. 2020. "The WRF-Hydro® modeling system technical description, (Version 5.2.0)". Technical report, NCAR Technical Note.

Kim, K. Y., W. Wu, E. Kutanoglu, J. J. Hasenbein, and Z. Yang. 2021. "Hurricane scenario generation for uncertainty modeling of coastal and inland flooding". *Frontiers in Climate* 3:16.

Kim, S.-H., and M. Shinozuka. 2004. "Development of fragility curves of bridges retrofitted by column jacketing". *Probabilistic Engineering Mechanics* 19(1):105–112. Fourth International Conference on Computational Stochastic Mechanics.

Kurtz, Z. D., C. L. Müller, E. R. Miraldi, D. R. Littman, M. J. Blaser, and R. A. Bonneau. 2015, 05. "Sparse and compositionally robust inference of microbial ecological networks". *PLOS Computational Biology* 11(5):1–25.

Logan, T. M., T. Aven, S. D. Guikema, and R. Flage. 2022, 09. "Risk science offers an integrated approach to resilience". *Nature Sustainability* 5(9):741–748.

Ma, X., Y. Sun, and H. Fang. 2013. "Scenario generation of wind power based on statistical uncertainty and variability". *IEEE Transactions on Sustainable Energy* 4(4):894–904.

Miura, Y., P. C. Dinenis, K. T. Mandli, G. Deodatis, and D. Bienstock. 2021. "Optimization of coastal protections in the presence of climate change". *Frontiers in Climate* 3:613293.

Morton, D., E. Popova, and I. Popova. 2006. "Efficient fund of hedge funds construction under downside risk measures". *Journal of Banking  Finance* 30(2):503–518. Risk Management and Optimization in Finance.

Panteli, M., C. Pickering, S. Wilkinson, R. Dawson, and P. Mancarella. 2017. "Power system resilience to extreme weather: fragility modeling, probabilistic impact assessment, and adaptation measures". *IEEE Transactions on Power Systems* 32(5):3747–3757.

Rota, M., A. Penna, and G. Magenes. 2010. "A methodology for deriving analytical fragility curves for masonry buildings based on stochastic nonlinear analyses". *Engineering Structures* 32(5):1312–1323.

Rüttgers, M., S. Jeon, S. Lee, and D. You. 2022. "Prediction of typhoon track and intensity using a generative adversarial network with observational and meteorological data". *IEEE Access* 10:48434–48446.

Smith, A.B. 2024. "U. S. billion-dollar weather and climate disasters, 1980 - present (NCEI Accession 0209268)".

Souto, L., J. Yip, W. Wu, B. Austgen, E. Kutanoglu, J. Hasenbein, Z. Yang, C. King, and S. Santoso. 2022. "Power system resilience to floods: modeling, impact assessment, and mid-term mitigation strategies". *International Journal of Electrical Power & Energy Systems* 135:107545.

Street, A., F. Oliveira, and J. M. Arroyo. 2011. "Contingency-constrained unit commitment with $n-K$ security criterion: a robust optimization approach". *IEEE Transactions on Power Systems* 26(3):1581–1590.

Sun, M., J. Cremer, and G. Strbac. 2018. "A novel data-driven scenario generation framework for transmission expansion planning with high renewable energy penetration". *Applied Energy* 228:546–555.

Villani, M., L. Sani, M. Amoretti, E. Vicari, R. Pecori, M. Mordonini, S. Cagnoni, and R. Serra. 2018. "A relevance index method to infer global properties of biological networks". In *Artificial Life and Evolutionary Computation*, edited by M. Pelillo, I. Poli, A. Roli, R. Serra, D. Slanzi, and M. Villani, 129–141. Cham: Springer International Publishing.

Wadman, W. S., Y. Kim, M. A. Lavin, S. Shukla, F. Heng, and U. Insights. 2017. "Deducing historical correlations for realistic stochastic forecasting of intermittent energy sources". In *2017 IEEE Power  Energy Society General Meeting*, 1–5.

Wang, Q., J. Watson, and Y. Guan. 2013. "Two-stage robust optimization for $N-k$ contingency-constrained unit commitment". *IEEE Transactions on Power Systems* 28(3):2366–2375.

Watson, J., R. Guttromson, C. Silva-Monroy, R. Jeffers, K. Jones, and J. Ellison *et al*. 2014, September. "Conceptual framework for developing resilience metrics for the electricity, oil, and gas sectors in the United States". Technical report, Sandia National Laboratories.

Zachry, B. C., W. J. Booth, J. R. Rhome, and T. M. Sharon. 2015. "A national view of storm surge risk and inundation". *Weather, Climate, and Society* 7(2):109–117.

## AUTHOR BIOGRAPHIES

**ASHUTOSH SHUKLA** is a Senior Operations Research and Advanced Analytics Specialist at BNSF Railway. Prior to joining BNSF Railway, he received his M.S. and Ph.D. from The University of Texas at Austin. Dr. Shukla's dissertation research focuses on the development of stochastic programming and robust optimization models for power grid resilience planning for extreme flood events. His email address is: ashutosh.shukla@utexas.edu.

**JOHN HASENBEIN** is a professor in the Graduate Program in OR/IE at the University of Texas Austin. He received his B.S. in Systems Science and Mathematics from Washington University in St. Louis and his M.S. and Ph.D. from Georgia Tech. Dr. Hasenbein's research interests include queueing and fluid models, large deviations, and Markov decision processes. He has done applied work in the areas of semiconductor scheduling, decision making in epilepsy treatment, hurricane evacuation, risk analysis in nuclear power plants, and power systems resilience. He is on the editorial boards of Operations Research, Queueing Systems, and Stochastic Systems. Dr. Hasenbein has been supported by NSF via an International Research Fellowship and a CAREER award, among other grants. His applied research projects have been funded by AMD, International Sematech, Samsung, Ayata, Zilliant, ConocoPhillips, the South Texas Nuclear Operating Company, and the DOE. His email address is: has@me.utexas.edu.

**ERHAN KUTANOGLU** is an Associate Professor of Operations Research and Industrial Engineering in the Cockrell School of Engineering at the University of Texas at Austin. His current research interests focus on infrastructure and community resilience planning and humanitarian logistics using large-scale modeling and optimization. His research seeks to combine predictive science-based models with prescriptive stochastic optimization models to develop an end-to-end understanding of uncertainty and optimized decision making, particularly for equitable climate adaptation and resilience planning. He holds a Ph.D. in Industrial Engineering from Lehigh University, is a recipient of NSF CAREER Award and IBM Faculty Award, and is an active member of INFORMS and IISE. His email address is: erhank@austin.utexas.edu.